

Safe Reinforcement Learning Using Black-Box Reachability Analysis

Mahmoud Selim¹, Amr Alanwar², Shreyas Kousik³, Grace Gao³, Marco Pavone³, and Karl H. Johansson⁴

Abstract—Reinforcement learning (RL) is capable of sophisticated motion planning and control for robots in uncertain environments. However, state-of-the-art deep RL approaches typically lack safety guarantees, especially when the robot and environment models are unknown. To justify widespread deployment, robots must respect safety constraints without sacrificing performance. Thus, we propose a Black-box Reachability-based Safety Layer (BRSL) with three main components: (1) data-driven reachability analysis for a black-box robot model, (2) a trajectory rollout planner that predicts future actions and observations using an ensemble of neural networks trained online, and (3) a differentiable polytope collision check between the reachable set and obstacles that enables correcting unsafe actions. In simulation, BRSL outperforms other state-of-the-art safe RL methods on a Turtlebot 3, a quadrotor, and a trajectory-tracking point mass with an unsafe set adjacent to the area of highest reward.

I. INTRODUCTION

In reinforcement learning (RL), an agent perceives consecutive states of its environment and acts after each observation to maximize long-term cumulative expected reward [1]. One key challenge to the widespread deployment of RL in safety-critical systems is the difficulty of ensuring that an RL agent’s policies are safe, especially when the system model and its surrounding environment are both unknown and subject to noise [2], [3], [4]. In this work, we consider the case of RL for guaranteed-safe navigation of mobile robots, such as autonomous cars or delivery drones, where safety means collision avoidance. We leverage the ability of an RL agent to plan complex sequences of actions in concert with data-driven reachability analysis to guarantee safety by post-processing the RL agent’s actions.

A. Related Work

Safety has long been of interest in RL research. Unlike traditional RL, Safe RL aims to learn policies that maximize expected reward on a task while respecting safety constraints during both learning and deployment [4]. Safe RL can be broadly classified as *objective-based* or *exploration-based*, depending on how safety is formulated. We first discuss these categories, then the specific case of mobile robot navigation, which we use to evaluate our proposed method.

Objective-based methods encourage safety by penalizing constraint violations in the objective. This can be done by

This work was supported by the Swedish Research Council, and the Knut and Alice Wallenberg Foundation. Toyota Research Institute provided funds to support this work.

¹Ain Shams University, Cairo, Egypt. ²Jacobs University, Bremen, Germany. ³Stanford University, Stanford, CA, USA. ⁴KTH Royal Institute of Technology, Stockholm, Sweden. Corresponding author: mahmoud.selim@eng.asu.edu.eg.

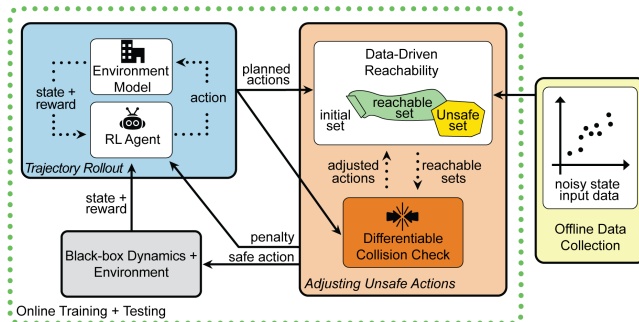


Fig. 1. Overview of the proposed BRSL method. Given data collected offline (in yellow, right), we perform online safe training and deployment of an RL agent. The RL agent creates trajectory plans for a robot in a receding-horizon way as follows, where each planning iteration is one clockwise loop in the green dashed box. First (in blue, top left), the agent predicts a possible future trajectory by rolling out its current policy with an ensemble of neural networks trained online to model the black-box environment (in grey, bottom left). Second (in orange, middle), the candidate plan is *adjusted* to ensure that it is safe using data-driven reachability and a novel constrained, differentiable method of collision-checking if our robot’s reachable sets are in collision. Finally, the new safe plan is passed to the robot, and a penalty is passed to the RL agent depending on how much the plan was adjusted.

relating cumulative reward to the system’s risk, such as the probability of visiting error states [5]. In practice, this results in an RL agent attempting to minimize an empirical risk measure (that is, an approximation of the probability of entering a dangerous or undesired state). Similarly, one can penalize the probability of losing reward (by visiting an unsafe state) for a given action [2], in which case the agent minimizes temporal differences in the reward and thus also minimizes risk. Another approach is to restrict policies to be ergodic with high probability, meaning any state can eventually be reached from any other state [6]. This is a more general problem, which comes at a cost: feasible safe policies do not always exist, and the algorithms are far more complex. While these methods can make an agent prefer safe actions, they cannot guarantee safety during training or deployment. Another group of objective-based algorithms aims to modify the Markov Decision Process (MDP) that the RL agent tries to optimize. Some model safe optimization problems as maximizing an unknown expected reward function [7]. However, they exploit regularity assumptions on the function wherein similar decisions are associated with similar rewards. They also assume the bandit setting, where decisions do not cause state transitions.

Others utilize constrained MDPs to enforce safety [8]. These can be broadly classified into two categories: Offline and Online. The offline approach [9], [10] collects the data

first then does the optimization. These are quite conservative and also are hard to scale. Online methods [11], [12], [13] on the other hand couples both the data collection and optimization. However, they don't guarantee safety in training.

Exploration-based methods modify the agent's exploration process instead of its optimization criterion. Exploration is the process of learning about unexplored states by trying random actions or actions that are not expected to yield maximum reward (for example, an ϵ -greedy strategy). However, visiting unexplored states naïvely can harm a robot or its environment. To avoid this, one can aim to guarantee safety during both exploration and exploitation, in both training and testing, by modifying the exploration strategy to incorporate risk metrics [14]. One can also use prior knowledge as an inductive bias for the exploration process [4], [15]; for example, one can provide a finite set of demonstrations as guidance on the task [16]. Although these approaches can provide strong safety guarantees, most of them assume prior knowledge on some or all components of the system model [17], [18], [19], which is not always feasible for more complicated systems. In addition, some techniques in this category also suffer the curse of dimensionality [18], [20].

Safe navigation is a fundamental problem in robotics. Classical techniques such as A* or RRT [21, Ch. 5] have been proposed to solve the navigation problem without learning. Safety in such techniques has been enforced at different levels of the planning hierarchy, such as trajectory planning [22], or low-level control [23]. More recently, however, learning-based methods have also been proposed [19], [18], [17]. Some safe RL navigation approaches depend on learning a value function of the expected time that an agent takes to reach the desired goal [24], [25]. Other approaches depend on learning the actions of the robot in an end-to-end manner [26], [27], [28], meaning that the agent attempts to convert raw sensor inputs (e.g., camera or LIDAR) into actuator commands. However, guaranteeing safety for robot navigation is generally challenging because robots typically have uncertain, nonlinear dynamics.

B. Proposed Method and Contributions

We propose a Black-box Reachability-based Safety Layer (BRSL), illustrated in Fig. 1, to enable strict safety guarantees for RL in an entirely data-driven way, addressing the above challenges of lacking robot and environment models *a priori* and of enforcing safety for uncertain systems. BRSL enforces safety by computing a system's forward reachable set, which is the union of all trajectories that the system can realize within a finite or infinite time when starting from a bounded set of initial states, subject to a set of possible input signals [29]. Then, if the reachable set does not intersect with unsafe sets, the system is verified as safe [22], [23], [30].

Limitations. Our method requires an approximation for the upper bound of a system's Lipschitz constant, similar to [19], [31], [32]. This results in a curse of dimensionality with respect to number of samples required to approximate the constant; note other sampling-based approaches scale

similarly [19], [18]. Furthermore, we focus on a discrete-time setting, assume our robot can brake to a stop, and assume accurate perception of the robot's surroundings. We leave continuous-time (which can be addressed with similar reachability methods to ours [18], [30]) and perception uncertainty to future work.

Contributions. We show the following with BRSL:

- 1) We extend a *differentiable polytope collision check* [33] to move reachable sets out of collision with obstacles.
- 2) We propose a safety layer by integrating the data-driven reachability analysis with the differentiable polytope collision check and a trajectory rollout planner.
- 3) We demonstrate BRSL on robot navigation, where it outperforms a baseline RL agent, Reachability-based Trajectory Safeguard (RTS) [18], and Safe Advantage-based Intervention for Learning policies with Reinforcement (SAILR) [34]. In particular, BRSL uses more efficient collision checking and online optimization than RTS, along with hard constraints, unlike SAILR.

Next, in Section II, we provide preliminaries and formulate our safe RL problem. Sections III and IV discuss and evaluate the proposed approach. Finally, Section V presents concluding remarks and discusses future work.

II. PRELIMINARIES AND PROBLEM FORMULATION

This section presents the notation, set representations, system dynamics, and reachable set definitions used in this work. We then pose our safe RL problem.

A. Notation and Set Representations

The n -dimensional real numbers are \mathbb{R}^n , the natural numbers are \mathbb{N} , and the integers from n to m are $n:m$. We denote the element at row i and column j of matrix \mathbf{A} by $(\mathbf{A})_{i,j}$ and column j of \mathbf{A} by $(\mathbf{A})_{:,j}$. The $\text{diag}(\cdot)$ operator places its arguments block-diagonally in a matrix of zeros. The Kronecker product is denoted \otimes . For a pair of sets A and B , the Minkowski sum is $A + B = \{\mathbf{a} + \mathbf{b} \mid \mathbf{a} \in A, \mathbf{b} \in B\}$, and the Cartesian product is denoted by $A \times B$.

We represent sets using constrained zonotopes, zonotopes, and intervals, because they enable efficient Minkowski sum computation (a key part of reachability analysis) [30] and collision checking via linear programming [35] (critical to safe motion planning). A *constrained zonotope* [35] is a convex set parameterized by a center $\mathbf{c} \in \mathbb{R}^n$, generator matrix $\mathbf{G} \in \mathbb{R}^{n \times n_g}$, constraint matrix $\mathbf{A} \in \mathbb{R}^{n_c \times n_g}$, and constraint vector $\mathbf{b} \in \mathbb{R}^{n_c}$ as

$$\mathcal{Z}(\mathbf{c}, \mathbf{G}, \mathbf{A}, \mathbf{b}) = \{\mathbf{c} + \mathbf{G}\mathbf{z} \mid \mathbf{A}\mathbf{z} = \mathbf{b}, \|\mathbf{z}\|_\infty \leq 1\}. \quad (1)$$

By [35, Thm. 1], every convex, compact polytope is a constrained zonotope and vice-versa. For polytopes represented as an intersection of halfplanes, we convert them to constrained zonotopes by finding a bounding box, then applying the halfspace intersection property in [36].

A zonotope is a special case of a constrained zonotope without equality constraints (but with $\|\mathbf{z}\|_\infty \leq 1$), which we denote $\mathcal{Z}(\mathbf{c}, \mathbf{G})$. For $Z = \mathcal{Z}(\mathbf{c}, \mathbf{G}) \subset \mathbb{R}^n$ and a linear map L , we have $LZ = \mathcal{Z}(L\mathbf{c}, L\mathbf{G})$; we denote $-Z = -1Z$. The Minkowski sum of two zonotopes $Z_1 =$

$\mathcal{Z}(\mathbf{c}_1, \mathbf{G}_1)$ and $Z_2 = \mathcal{Z}(\mathbf{c}_2, \mathbf{G}_2)$ is given by $Z_1 + Z_2 = \mathcal{Z}(\mathbf{c}_1 + \mathbf{c}_2, [\mathbf{G}_1, \mathbf{G}_2])$ [30]. For an n -dimensional interval with lower (resp. upper) bounds $\underline{\mathbf{l}} \in \mathbb{R}^n$ (resp. $\bar{\mathbf{l}}$), we abuse notation to represent it as a zonotope $Z = \mathcal{Z}(\underline{\mathbf{l}}, \bar{\mathbf{l}}) \subset \mathbb{R}^n$, with center $\frac{1}{2}(\underline{\mathbf{l}} + \bar{\mathbf{l}})$ and generator matrix $\text{diag}(\frac{1}{2}(\bar{\mathbf{l}} - \underline{\mathbf{l}}))$.

B. Robot and Environment

We assume the robot can be described as a discrete-time, Lipschitz continuous, nonlinear control system with state $\mathbf{x}_k \in X \subset \mathbb{R}^n$ at time $k \in \mathbb{N}$. We assume the state space X is compact. The input \mathbf{u}_k is drawn from a zonotope $U_k \subseteq U$ at each time k , where $U \subset \mathbb{R}^m$ is a zonotope of all possible actions. We denote process noise by $\mathbf{w}_k \in W \subset \mathbb{R}^n$, where W is specified later in Assumption 2. Finally, we denote the (black box) dynamics $\mathbf{f} : X \times U \times W \rightarrow X$, for which

$$\mathbf{x}_{k+1} = \mathbf{f}(\mathbf{x}_k, \mathbf{u}_k) + \mathbf{w}_k. \quad (2)$$

We further assume that \mathbf{f} is twice differentiable. We denote the initial state of the system as \mathbf{x}_0 , drawn from a compact set $X_0 \subset \mathbb{R}^n$. Note that this formulation leads to an MDP.

To enable safety guarantees, we leverage the notion of failsafe maneuvers from mobile robotics [22], [37].

Assumption 1. *We assume the dynamics \mathbf{f} are invariant to translation in position, and the robot can brake to a stop in $n_{\text{brk}} \in \mathbb{N}$ time steps and stay stopped indefinitely. That is, there exists $\mathbf{u}_{\text{brk}} \in U$ such that, if the robot is stopped at state \mathbf{x}_k , and if $\mathbf{x}_{k+1} = \mathbf{f}(\mathbf{x}_k, \mathbf{u}_{\text{brk}})$, then $\mathbf{x}_{k+1} = \mathbf{x}_k$.*

Note, many real robots have a braking safety controller available, similar to the notion of an invariant set [19], [18].

We require that process noise obeys the following assumption for numerical tractability and robustness guarantees.

Assumption 2. *Each \mathbf{w}_k is drawn uniformly from a noise zonotope $W = \mathcal{Z}(\mathbf{c}_w, \mathbf{G}_w)$ with $n_{g,w}$ generators.*

This formulation does not handle discontinuous changes in noise. However, there exist zonotope-based techniques to identify a change in W [38], after which one can compute the system’s reachable set as in this work. We leave measurement noise and perception uncertainty to future work.

We denote unsafe regions of state space, or *obstacles*, as $X_{\text{obs}} \subset X$. We assume obstacles are static but different at each episode, as the focus of this work is not on predicting other agents’ motion. Reachability-based frameworks exist to handle other agents’ motion [23], [39], so the present work can extend to dynamic environments. We further assume the robot can instantaneously sense all obstacles (that is, X_{obs}) and represent them as a union of constrained zonotopes. We also note that common obstacle representations, such as occupancy grids, are polygonal, so they can be represented as constrained zonotopes. In the case of sensing limits, one can determine a minimum distance within which obstacles must be detected to ensure safety, given a robot’s maximum speed and braking distance [22, Section 5].

C. Reachable Sets

We ensure safety by computing our robot’s forward reachable set (FRS) for a given motion plan, then adjusting the

Algorithm 1: Safe RL with BRSL

```

1 initialize the RL agent with a random policy  $\pi_\theta$ ,
   environment model  $\mu_\phi$ , empty replay buffer  $B$ , max
   number of time steps  $n_{\text{iter}}$ , and a safe plan  $\mathbf{p}_0$ 
2 for each episode do
3   initialize task with reward function  $\rho$ 
4    $\hat{\mathbf{x}}_1 \leftarrow$  observe initial environment state
5   for  $k = 1 : n_{\text{iter}}$  do
6      $\mathbf{p}_k \leftarrow$  roll out a trajectory
7      $\hat{R}_k \leftarrow \mathcal{Z}(\mathbf{x}_k, \mathbf{0})$  // init. reachable set
8      $(\hat{R}_j)_{j=k}^{k+n_{\text{plan}}} \leftarrow \text{reach}(\hat{R}_k, \mathbf{p}_k)$  // use Alg. 2
9     if any  $\hat{R}_j \cap X_{\text{obs}} \neq \emptyset$  then
10      try  $\mathbf{p}_k \leftarrow \text{adjust}(\mathbf{p}_k, X_{\text{obs}})$  // use Alg. 3
11      catch execute failsafe maneuver; continue
12      $\mathbf{u}_k \leftarrow$  get first (safe) action from  $\mathbf{p}_k$ 
13      $r_k \leftarrow \rho(\hat{\mathbf{x}}_k, \mathbf{u}_k)$  // get reward
14      $\hat{\mathbf{x}}_{k+1} \leftarrow$  observe next environment state
15     add  $(\hat{\mathbf{x}}_k, \mathbf{u}_k, r_k, \hat{\mathbf{x}}_{k+1})$  to  $B$ 
16     train the RL agent  $\pi_\theta$  and the environment
       model  $\mu_\phi$  using minibatch from  $B$ 

```

plan so that the FRS lies outside of obstacles. We define the FRS, henceforth called the reachable set, as follows:

Definition 1. *The reachable set R_k at time step k , subject to a sequence of inputs $\mathbf{u}_j \in U_j \subset \mathbb{R}^m$, noise $\mathbf{w}_j \in W \forall j \in \{0, \dots, k-1\}$, and initial set $X_0 \in \mathbb{R}^n$, is the set*

$$R_k = \{ \mathbf{x}_k \in \mathbb{R}^n \mid \mathbf{x}_{j+1} = \mathbf{f}(\mathbf{x}_j, \mathbf{u}_j) + \mathbf{w}_j, \mathbf{x}_0 \in X_0, \mathbf{u}_j \in U_j, \text{ and } \mathbf{w}_j \in W, \forall j = 0, \dots, k-1 \}. \quad (3)$$

Recall that we treat the dynamics \mathbf{f} as a black box (e.g., a simulator), which could be nonlinear and difficult to model, but we still seek to conservatively approximate (that is, overapproximate) the reachable set R_k . Doing so requires conservatively estimating the Lipschitz constant of the dynamics, as is done in the literature [31], [32].

D. Safe RL Problem Formulation

We denote the state of the RL agent at time k by $\hat{\mathbf{x}}_k \in \mathbb{R}^{n_{\text{RL}}}$, which contains the state \mathbf{x}_k of the robot plus information such as sensor measurements and previous actions. At each time k , the RL agent chooses \mathbf{u}_k . Recall that $X_{\text{obs}} \subset \mathbb{R}^n$ denotes obstacles. For a given task, we construct a reward function $\rho : (\hat{\mathbf{x}}_k, \mathbf{u}_k) \mapsto r_k \in \mathbb{R}$ (examples of ρ are given in Section IV). At time k , let $\mathbf{p}_k = (\mathbf{u}_j)_{j=k}^{n_{\text{plan}}}$ denote a *plan*, or sequence of actions, of duration $n_{\text{plan}} \in \mathbb{N}$.

Then, our safe RL problem is as follows. We seek to learn a policy $\pi_\theta : \hat{\mathbf{x}}_k \mapsto \mathbf{u}_k$, represented by a neural network with parameters θ , that maximizes expected cumulative reward. Note that the policy can be deterministic or stochastic. Since rolling out the policy may lead to collisions, we also seek to create a safety layer between the policy and the robot (that is, to ensure $R_j \cap X_{\text{obs}} = \emptyset$ for all $j \geq k$).

III. BLACK-BOX REACHABILITY-BASED SAFETY LAYER

We now present our proposed BRS�, then detail the used data-driven reachability, and a method for adjusting unsafe actions. The key contribution is summarized in Theorem 1.

BRS� is summarized in Algorithm 1. It uses a receding-horizon strategy to create a new safe plan \mathbf{p}_k in each k^{th} receding-horizon motion planning iteration. Consider a single planning iteration (that is, time step k) (Lines 4–16). Suppose the RL agent has previously created a safe plan \mathbf{p}_{k-1} (such as staying stopped indefinitely). At the beginning of the iteration, BRS� creates a new plan \mathbf{p}_k by rolling out the RL agent along with an environment model. Next, BRS� chooses a safe action by adjusting the rolled-out action sequence (Lines 9–11) such that the corresponding reachable set (computed with Algorithm 2) is collision-free and ends with a failsafe maneuver. If the adjustment procedure (as in Algorithm 3) fails to find a safe plan, then the robot executes the failsafe maneuver. Finally, BRS� sends the first action in the current safe plan to the robot, gets a reward, and trains the RL agent and environment model (Lines 12–16). To enable training our environment model online, we collect data in a replay buffer B at each time k (Line 15). We note that BRS� can be used during both training and deployment. That is, the safety layer can operate even for an untrained policy. Thus, for training, we initialize π_θ with random weights.

A. Data-Driven Reachability Analysis

BRS� performs data-driven reachability analysis of a plan $\mathbf{p}_k = (\mathbf{u}_j)_{j=k}^{n_{\text{plan}}}$ using Algorithm 2, based on [32]. We now describe our offline data collection, then the algorithm.

Our reachability analysis uses noisy trajectory data of the black-box system model collected offline; we use data collected online only for training the policy and environment model. We consider q input-state trajectories of lengths $t_i \in \mathbb{N}$, $i = 1, \dots, q$, with total duration $t_{\text{total}} = \sum_i t_i$. We denote the data as $(\mathbf{x}_k^{(i)})_{k=0}^{t_i}$, $(\mathbf{u}_k^{(i)})_{k=0}^{t_i-1}$, $i = 1, \dots, q$, which we collect in matrices:

$$\mathbf{X}_- = \begin{bmatrix} \mathbf{x}_0^{(1)}, \dots, \mathbf{x}_{t_1-1}^{(1)}, \mathbf{x}_0^{(2)}, \dots, \mathbf{x}_0^{(q)}, \dots, \mathbf{x}_{t_q-1}^{(q)} \end{bmatrix}, \quad (4a)$$

$$\mathbf{X}_+ = \begin{bmatrix} \mathbf{x}_1^{(1)}, \dots, \mathbf{x}_{t_1}^{(1)}, \mathbf{x}_1^{(2)}, \dots, \mathbf{x}_1^{(q)}, \dots, \mathbf{x}_{t_q}^{(q)} \end{bmatrix}, \quad (4b)$$

$$\mathbf{U}_- = \begin{bmatrix} \mathbf{u}_0^{(1)}, \dots, \mathbf{u}_{t_1-1}^{(1)}, \mathbf{u}_0^{(2)}, \dots, \mathbf{u}_0^{(q)}, \dots, \mathbf{u}_{t_q-1}^{(q)} \end{bmatrix}. \quad (4c)$$

We collect all the data in a tuple $D = (\mathbf{X}_-, \mathbf{X}_+, \mathbf{U}_-)$. Selecting enough data to sufficiently capture system behavior is a challenge that depends on the system, though specific sampling strategies exist for some systems [18].

We must approximate the Lipschitz constant of the dynamics for our reachability analysis, which we do from the data D with the method in [32, Section 4, Remark 1]. We also require a data covering radius δ such that, for any data point $z_1 \in X \times U$, there exists another data point $z_2 \in X \times U$ for which $\|z_1 - z_2\|_2 \leq \delta$. We assume a sufficiently large number of data points is known *a priori* to upper-bound L^* and lower-bound δ ; and, we assume L^* and δ are the same for offline data collection and online operation. Note, prior work also assumes similar bounds [31], [32].

Algorithm 2: Black-box System Reachability [32]

Input: initial reachable set \hat{R}_0 , actions $(\mathbf{u}_j)_{j=k}^{k+n_{\text{plan}}}$
Parameter: state/action data D , noise zonotope $W = \mathcal{Z}(\mathbf{c}_w, \mathbf{G}_w)$, Lipschitz constant L^* , and covering radius δ

- 1 $Z_\epsilon \leftarrow \mathcal{Z}(\mathbf{0}, \text{diag}(L^*\delta, \dots, L^*\delta))$
- 2 **for** $j = k : (k + n_{\text{plan}})$ **do**
- 3 $\mathbf{M}_j \leftarrow (\mathbf{X}_+ - [\mathbf{c}_w, \dots, \mathbf{c}_w]) \begin{bmatrix} \mathbf{1}_{1 \times t_{\text{total}}} \\ \mathbf{X}_- - \mathbf{1} \otimes \mathbf{x}_j^* \\ \mathbf{U}_- - \mathbf{1} \otimes \mathbf{u}_j \end{bmatrix}^\dagger$
- 4 $\underline{\mathbf{l}} \leftarrow \min_j \left((\mathbf{X}_+)_{:,j} - \mathbf{M}_j \begin{bmatrix} \mathbf{1} \\ (\mathbf{X}_-)_{:,j} - \mathbf{x}_j^* \\ (\mathbf{U}_-)_{:,j} - \mathbf{u}_j \end{bmatrix} \right)$
- 5 $\bar{\mathbf{l}} \leftarrow$ same as $\underline{\mathbf{l}}$, but use max instead of min
- 6 $Z_L \leftarrow \mathcal{Z}(\underline{\mathbf{l}}, \bar{\mathbf{l}}) - W$ and $U_j \leftarrow \mathcal{Z}(\mathbf{u}_j, \mathbf{0})$
- 7 $\hat{R}_{j+1} \leftarrow \mathbf{M}_j(\mathbf{1} \times \hat{R}_j \times U_j) + W + Z_L + Z_\epsilon$.
- 8 **return** $(\hat{R}_j)_{j=k}^{k+n_{\text{plan}}}$ // overapproximates (3)

We summarize our online reachability approach in Algorithm 2, which overapproximates the reachable set as in (3) by computing a zonotope $\hat{R}_j \supseteq R_j$ for each time step of the current plan. First we compute a Lipschitz zonotope Z_ϵ (Line 1). Then, for each time step, we compute a least-squares model (Line 3) at a linearization point $(\mathbf{x}_j^*, \mathbf{u}_j^*)$, where \mathbf{x}_j^* is the center of the current reachable set zonotope as per [30], [32]. Next, we overapproximate model mismatch and nonlinearity as a zonotope using the noise zonotope W from Assumption 2 (Lines 5–6). Finally, we perform a reachability step using the previously computed zonotopes (Line 7).

The black-box system data strongly affects the conservativeness of the reachable set, which can worsen over many timesteps. This is because L^* and δ are approximated from the data for use in Algorithm 2. We mitigate conservativeness by leveraging the dynamics’ translation invariance to rescale the state space to $[0, 1]^n$, which we found works empirically.

B. Adjusting Unsafe Actions

After the RL agent rolls out a plan \mathbf{p}_k , the safety layer determines if it is safe by checking the intersection of the corresponding reachable sets with unsafe sets. Note, the adjustment procedure does not depend on π_θ , only on the unsafe sets around the robot. The plan is applied to the environment if the action is deemed safe; otherwise, we look for a safe plan. One strategy for finding a safe plan is to sample randomly in the action space [18], but this can be prohibitively expensive in the large action spaces that arise from choosing control inputs at multiple time steps. Instead, we use gradient descent to *adjust* our plan such that the reachable sets are not in a collision, and such that the plan has a failsafe maneuver.

We adjust unsafe actions using Algorithm 3. If the algorithm does not complete within the duration of one time step (in other words, we fix the rate of receding-horizon planning), we terminate it and continue our previously-found safe plan. Our method steps through each action in a plan \mathbf{p}

and performs the following. First, we compute the reachable set for all remaining time steps with Algorithm 2 (Line 5). Second, we collision check the reachable set (Line 6) as detailed below. Third, if the reachable sets are in a collision, we compute the gradient of the collision check and perform projected gradient descent (Line 8). Finally, if the algorithm converges to a safe plan, we return it, or else return “unsafe.” Note, the final plan must have a failsafe maneuver (Line 11).

We collision check reachable and unsafe sets, all represented as constrained zonotopes, as follows. Consider two constrained zonotopes, $Z_1 = \mathcal{Z}(\mathbf{c}_1, \mathbf{G}_1, \mathbf{A}_1, \mathbf{b}_1)$ and $Z_2 = \mathcal{Z}(\mathbf{c}_2, \mathbf{G}_2, \mathbf{A}_2, \mathbf{b}_2)$. Applying [35, Prop. 1], their intersection is $Z_\cap = Z_1 \cap Z_2 = \mathcal{Z}(\mathbf{c}_\cap, \mathbf{G}_\cap, \mathbf{A}_\cap, \mathbf{b}_\cap)$, given by

$$Z_\cap = \mathcal{Z} \left(\mathbf{c}_\cap, [\mathbf{G}_1, \mathbf{0}], \begin{bmatrix} \mathbf{A}_1 & \mathbf{0} \\ \mathbf{0} & \mathbf{A}_2 \\ \mathbf{G}_1 & -\mathbf{G}_2 \end{bmatrix}, \begin{bmatrix} \mathbf{b}_1 \\ \mathbf{b}_2 \\ \mathbf{c}_2 - \mathbf{c}_1 \end{bmatrix} \right). \quad (5)$$

We check if $Z_1 \cap Z_2$ is empty by solving a linear program, as per [35, Prop. 2]:

$$v^* = \min_{\mathbf{z}, v} \{v \mid \mathbf{A}_\cap \mathbf{z} = \mathbf{b}_\cap \text{ and } |\mathbf{z}| \leq v\}, \quad (6)$$

with $|\mathbf{z}|$ taken elementwise; Z_\cap is nonempty iff $v \leq 1$. Note, (6) is feasible when Z_1 and Z_2 have feasible constraints.

We use gradient descent to move our reachable sets \hat{R}_k out of collision. Since we use (6) for collision checking, we differentiate its solution with respect to the problem parameters using [40], [33]. Let $\hat{\mathbf{c}}_k$ denote the center of \hat{R}_k . Per Algorithm 2, \hat{R}_k is a function of $\mathbf{u}_0, \dots, \mathbf{u}_{k-1}$. Let (\mathbf{z}^*, v^*) be an optimal solution to (6) when the problem parameters (i.e., the input constrained zonotopes) are \hat{R}_k and an unsafe set. Collision avoidance requires $v^* > 1$ [35, Prop. 2]. We compute the gradient $\nabla_{\mathbf{u}_k} v^*$ with respect to the input action (assuming a constant linearization point) using a chain rule recursion with $i = 0, \dots, n_{\text{plan}}$ given by

$$\nabla_{\mathbf{u}_{k-i}} v^* = \nabla_{\hat{\mathbf{c}}_k} v^* \nabla_{\hat{\mathbf{c}}_{k-1}} \hat{\mathbf{c}}_k \left(\prod_{j=k-i+2}^{j=k-1} \nabla_{\hat{\mathbf{c}}_{j-1}} \hat{\mathbf{c}}_j \right) \nabla_{\mathbf{u}_{k-i}} \hat{\mathbf{c}}_{k-i+1}, \quad (7a)$$

$$\nabla_{\hat{\mathbf{c}}_{k-1}} \hat{\mathbf{c}}_k = (\mathbf{M}_{k-1})_{(1:1+n), (1:1+n)}, \quad \text{and} \quad (7b)$$

$$\nabla_{\mathbf{u}_{k-1}} \hat{\mathbf{c}}_k = (\mathbf{M}_{k-1})_{:, (n+1:n+1+m)} \quad (7c)$$

where \mathbf{M}_{k-1} is computed as in Algorithm 2, Line 3, and n and m are the state and action dimensions. After using $\nabla_{\mathbf{u}_k} v^*$ for gradient descent on \mathbf{u}_k , we project \mathbf{u}_k to the set of feasible controls: $\text{proj}_{U_k}(\mathbf{u}_k) = \arg \min_{\mathbf{v} \in U_k} \{\|\mathbf{u}_k - \mathbf{v}\|_2^2\}$. The resulting control may be unsafe, so we collision-check the final reachable sets at the end of Algorithm 3.

C. Analyzing Safety

We conclude this section by formalizing the notion that BRS� enables safe RL.

Theorem 1. *Suppose the assumptions on the robot and environment from Section II all hold, and, at time $k = 0$, the robot is stationary. Suppose also that, at each time $k > 0$, the robot rolls out a new \mathbf{p}_k , then adjusts the plan using*

Algorithm 3: Adjusting Unsafe Actions

Input: plan $\mathbf{p}_k = (\mathbf{u}_j)_{j=k}^{n_{\text{plan}}}$, obstacles X_{obs} , initial reachable set \hat{R}_k , step size γ , time limit t_{max} , time steps required to stop n_{brk}

- 1 // note \mathbf{p}_k has failsafe \mathbf{u}_{brk} for all $j > k + n_{\text{plan}}$
- 2 $\mathbf{p}_{\text{safe}} \leftarrow \mathbf{p}_k$ // initialize with given plan
- 3 **for** $j = k : (k + n_{\text{plan}} + n_{\text{brk}})$ **do**
- 4 **while** *time limit not exceeded* **do**
- 5 $(\hat{R}_j)_{j=k}^{k+n_{\text{plan}}} \leftarrow \text{reach}(\hat{R}_j, \mathbf{p}_{\text{safe}})$ // use Alg. 2
- 6 $v^* \leftarrow$ collision check $\hat{R}_j \cap X_{\text{obs}}$ using (6)
- 7 **if** $v^* \leq 1$ (i.e., in collision) **then**
- 8 $\mathbf{u}_j \leftarrow \text{proj}_{U_j}(\mathbf{u}_j + \gamma \nabla_{\mathbf{u}_j} v^*)$ // using (7)
- 9 **else**
- 10 **break** and restart inner while loop
- 11 **if** all $\hat{R}_j \cap X_{\text{obs}} = \emptyset$ and \mathbf{x}_n is stopped **then**
- 12 **return** $\mathbf{p}_{\text{safe}} = (\mathbf{u}_j)_{j=k}^{n_{\text{plan}}}$ // found new safe plan
- 13 **else**
- 14 **return** error “unsafe” // failed to find safe plan

Algorithm 3. Then, the robot is guaranteed to be safe at all times $k \geq 0$.

Proof. We prove the claim by induction on k . At time 0, the robot can apply \mathbf{u}_{brk} to stay safe for all time. Assume a safe plan exists at time $k \in \mathbb{N}$. Then, if the output of Algorithm 3 is unsafe (no new plan found), the robot can continue its previous safe plan; otherwise, if a new plan is found, the plan is safe for three reasons. First, the black-box reachability in Algorithm 2 is guaranteed to contain the true reachable set of the system [32, Theorem 2], because process noise is bounded by a zonotope as in Assumption 2. Second, when adjusting an unsafe plan with Algorithm 3, the zonotope collision check is guaranteed to always detect collisions [35, Prop. 2] to assess if $\hat{R}_j \cap X_{\text{obs}}$ is empty for each time step j of the plan. Third, Algorithm 3 requires that, after n_{plan} timesteps, the robot is stopped, so the new plan contains a failsafe maneuver, and the robot can safely apply \mathbf{u}_{brk} for all time $j \geq k + n_{\text{plan}}$. \square

IV. EVALUATION

We demonstrate BRS� on two types of environments: safe robot navigation to a goal (on a Turtlebot in Gazebo and on a quadrotor platform in Unreal Engine 4), and path following (in a point mass environment based on [9], [34]). All code is run on a desktop computer with an Intel i5 11600 CPU and a RTX 3060 GPU. We aim to assess the following:

- How does BRS� compare against a vanilla baseline (unsafe) RL agent and other safe RL methods (RTS [18] and SAILR [34]) in terms of reward and safety?
- How conservative is BRS� in environments where high reward states are near unsafe regions?
- Can BRS� actually be implemented in real time for safety-critical systems?

Setup. We use TD3 [41] as our RL agent, after determining empirically that it outperforms SAC [42] and DDPG [43]. We initialize the policy with random weights. Since the agent outputs continuous actions, to aid the exploration process, we inject zero-mean Gaussian noise with a variance of 0.5 that is dampened by a factor of 0.99995 per time step. Note that this strategy does not affect safety since our safety layer adjusts the output of the RL agent.

For each robot, to perform reachability analysis with Algorithm 2, we collect 500 time steps of noisy state/input data (as per (4)) offline in an empty environment while applying random control inputs. We found this quantity of data sufficient to ensure safety empirically; we leave a formal analysis of the minimum amount of data for future work.

We parameterize the environment model as an ensemble of neural networks, each modeling a Gaussian distribution over future states and observations. Each network has 4 layers, with hidden layers of size 200, and leaky ReLU activations with a negative slope of 0.01. We use a stochastic model for this ensemble, meaning that the ensemble predicts the parameters of a probability distribution, which is then sampled to produce a state as in [44].

Goal-Based Environments. For the Turtlebot 3, and the quadrotor the task is to navigate to a random circular goal region $X_{\text{goal}} \subset X$ while avoiding randomly-generated obstacles $X_{\text{obs}} \subset X$. Each robot starts in a safe location at the center of the obstacle map. Each task is episodic; an episode ends if the robot reaches the goal, crashes, or exceeds a time limit. Both robots have uncertain, noisy dynamics as in (2). We discretize time at 10 Hz.

The Turtlebot’s control inputs are longitudinal velocity in $[0.00, 0.25]$ m/s and angular velocity in $[-0.5, 0.5]$ rad/s (these are the bounds of U_k). The robot has wheel encoders, plus a planar lidar that generates 18 range measurements evenly spaced in a 180° arc in front of the robot. The robot requires $n_{\text{brk}} = 6$ time steps to stop, so we set $n_{\text{plan}} = 8$.

The quadrotor control inputs are commanded velocities up to 5 m/s in each spatial direction at each time step. The robot is equipped with an IMU and a 16-channel lidar which receives range measurements around the robot in a 50° vertical arc and a 360° horizontal arc. The robot has $n_{\text{brk}} = 10$, so we set $n_{\text{plan}} = 11$.

We use the following reward for goal-based environments:

$$\begin{aligned} \rho(\hat{\mathbf{x}}_k, \mathbf{u}_k) = & + 10^3 \cdot \mathbb{I}(\mathbf{x}_k \in X_{\text{goal}}) + \\ & - 20 \cdot d(\mathbf{x}_k, X_{\text{goal}}) + \\ & - 10^3 \cdot \mathbb{I}(\mathbf{u}_k \text{ is unsafe}), \end{aligned} \quad (8)$$

where $\mathbb{I}(\cdot)$ returns 1 if its argument is true or 0 otherwise, $d(\cdot, X_{\text{goal}})$ returns the Euclidean distance to the center of the goal region, and the safety of \mathbf{u}_k is checked using the reachable set of the RL agent’s plan (before adjustment). The robot position is estimated from the odometry of the robot.

Path Following Environments. The goal for the point robot is to follow a circular path of radius r as quickly as possible while constrained to a region smaller than the target circle. This lets us assess how conservative BRSL is because the

area of highest reward is closest to the unsafe set.

The point robot is a linear 2-D double integrator with position and velocity as its state: $\mathbf{x}_k = (x_k, y_k, \dot{x}_k, \dot{y}_k)$. It has a maximum velocity of 2 m/s, and its control input is acceleration up to 1 m/s² in any direction. We use these dynamics as they are from the safe RL literature [9], [34] and enable a fair test against other safety methods that require a robot model. We define a box-shaped safe set (the complement of the obstacle set) as $X_{\text{safe}} = \{\mathbf{x}_k \in X : |x_k| \leq x_{\text{max}}, |y_k| \leq y_{\text{max}}\}$, with $\|(x_{\text{max}}, y_{\text{max}})\|_2 < r$. We use a reward that encourages traveling quickly near the unsafe set:

$$\rho(\hat{\mathbf{x}}_k, \mathbf{u}_k) = \frac{(\dot{x}_k, \dot{y}_k) \cdot (-y_k, x_k)}{1 + \|(x_k, y_k)\|_2 - r}. \quad (9)$$

Results and Discussion. The results are summarized in Tables I (Goal-Based) and II (Path Following), and in Figure 2. In answer to the questions at the beginning of this section, BRSL outperforms the other methods in terms of reward and safety, is not overly conservative, and can operate in real time. However, SAILR and the baseline RL agent achieved higher speeds. Critically, both BRSL and RTS are safe, whereas SAILR and the baseline experience collisions (as expected). We note, BRSL accumulates higher reward than RTS, SAILR, and the baseline, while ensuring safety, and without a model of the robot *a priori*.

BRSL consistently replans faster than the 10 Hz time discretization, so it is capable of real-time operation. We note, RTS’ planning time increases with state space dimension, because it computes halfspace representation of zonotopes for collision checking [18], which is exponential in a zonotope’s number of generators [30]; we avoid this by using (6). It is possible RTS and SAILR can be made more computationally efficient with hyperparameter tuning; our focus is BRSL’s real-time capability.

We explain BRSL’s performance advantages as follows. First BRSL outputs a sequence of control actions, whereas RTS must choose from a low-dimensional parameterized set of possible plans, meaning BRSL is more flexible. Second, in contrast to SAILR, though both adjust unsafe actions, BRSL enforces hard constraints on safety. Finally, we note the quantity of data for BRSL determines the computation time of \mathbf{M}_j from Algorithm 2, which is used for reachability and adjusting unsafe actions. Therefore, one can ensure the amount of data allows real time operation; choosing the data optimally is left to future work.

V. CONCLUSION

This paper proposes the Black-box Reachability Safety Layer, or BRSL, a safety framework that does not require a system model and instead learns a stochastic model of the environment and robot online. BRSL ensures safety via data-driven reachable set computation paired with a novel technique to ensure collision-free reachable sets. The proposed framework was evaluated on three robot motion planning problems, which demonstrated that BRSL respects safety constraints while achieving a high reward over time in comparison to other state-of-the-art methods. For future

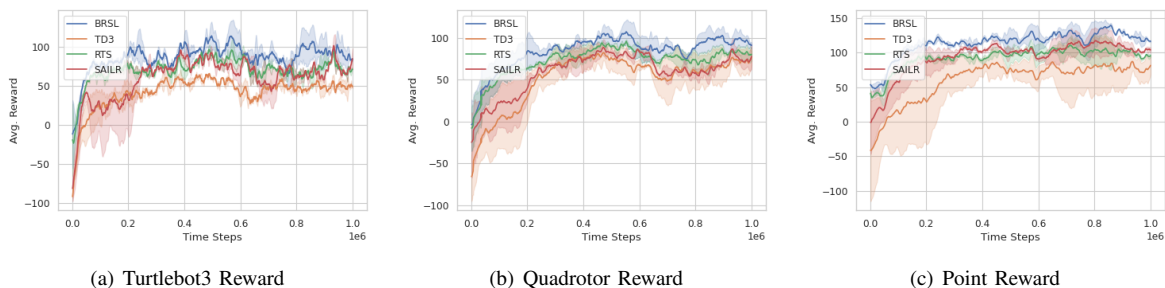


Fig. 2. Average reward over time of BRSL, RTS [18], SAILR [34], and a vanilla TD3 baseline for each of our experiments.

TABLE I
GOAL-BASED EXPERIMENT RESULTS (BEST VALUES IN BOLD)

| | Turtlebot | | | | Quadrotor | | | |
|--|-------------------|-------------------|------------------|-------------------------------------|-------------------|---------------------|-------------------|------------------------------------|
| | BRSL | RTS | SAILR | Baseline | BRSL | RTS | SAILR | Baseline |
| Goal Rate [%] | 57 | 52 | 48 | 42 | 76 | 66 | 61 | 54 |
| Collision Rate [%] | 0.0 | 0.0 | 7.3 | 48 | 0.0 | 0.0 | 9.2 | 59 |
| Mean/Max Speed [m/s] | .07 / 0.18 | 0.05 / 0.15 | .07 / 0.17 | .08 / .18 | 3.6 / 7.9 | 3.3 / 7.8 | 3.7 / 7.9 | 3.7 / 7.9 |
| Mean Reward | 86 | 78 | 68 | 63 | 82 | 73 | 61 | 57 |
| Mean \pm Std. Dev. Compute Time [ms] | 50.41 \pm 20.5 | 100.74 \pm 60.5 | 30.53 \pm 10.8 | 10.21 \pm 10.05 | 60.33 \pm 20.34 | 260.85 \pm 140.67 | 45.31 \pm 20.84 | 20.63 \pm 30.2 |

TABLE II
PATH FOLLOWING RESULTS (BEST RESULTS IN BOLD)

| | BRSL | RTS | SAILR | Baseline |
|-------------------|-----------------|-------------------|-------------------|-----------------------------------|
| Collisions [%] | 0.0 | 0.0 | 4.9 | 11.4 |
| Mean Speed [m/s] | 0.76 | 0.72 | 0.78 | 0.86 |
| Max Speed [m/s] | 2.00 | 1.89 | 2.00 | 2.00 |
| Mean Reward | 118 | 93 | 88 | 73 |
| Compute Time [ms] | 30.0 \pm 10.2 | 60.18 \pm 20.09 | 20.49 \pm 10.34 | 8.64 \pm 1.14 |

work, we will explore continuous-time settings and different representations for less conservative reachability, and the minimum amount of data needed for safety guarantees.

REFERENCES

- [1] R. S. Sutton, A. G. Barto, *et al.*, *Introduction to reinforcement learning*, vol. 135. MIT press Cambridge, 1998.
- [2] O. Mihatsch and R. Neuneier, “Risk-sensitive reinforcement learning,” *Machine learning*, vol. 49, no. 2, pp. 267–290, 2002.
- [3] R. Koppejan and S. Whiteson, “Neuroevolutionary reinforcement learning for generalized control of simulated helicopters,” *Evolutionary intelligence*, vol. 4, no. 4, pp. 219–241, 2011.
- [4] J. Garcia and F. Fernández, “A comprehensive survey on safe reinforcement learning,” *Journal of Machine Learning Research*, vol. 16, no. 1, pp. 1437–1480, 2015.
- [5] P. Geibel and F. Wysotzki, “Risk-sensitive reinforcement learning applied to control under constraints,” *Journal of Artificial Intelligence Research*, vol. 24, pp. 81–108, 2005.
- [6] T. M. Moldovan and P. Abbeel, “Safe exploration in markov decision processes,” 2012.
- [7] Y. Sui, A. Gotovos, J. Burdick, and A. Krause, “Safe exploration for optimization with gaussian processes,” in *Proceedings of the 32nd International Conference on Machine Learning (F. Bach and D. Blei, eds.)*, vol. 37 of *Proceedings of Machine Learning Research*, (Lille, France), pp. 997–1005, PMLR, 07–09 Jul 2015.
- [8] E. Altman, *Constrained Markov decision processes: stochastic modeling*. Routledge, 1999.
- [9] J. Achiam, D. Held, A. Tamar, and P. Abbeel, “Constrained policy optimization,” 2017.
- [10] H. Bharadhwaj, A. Kumar, N. Rhinehart, S. Levine, F. Shkurti, and A. Garg, “Conservative safety critics for exploration,” 2021.
- [11] V. Borkar, “An actor-critic algorithm for constrained markov decision processes,” *Systems & Control Letters*, vol. 54, no. 3, pp. 207–213, 2005.
- [12] Y. Chow, M. Ghavamzadeh, L. Janson, and M. Pavone, “Risk-constrained reinforcement learning with percentile risk criteria,” 2017.
- [13] S. Bohez, A. Abdolmaleki, M. Neunert, J. Buchli, N. Heess, and R. Hadsell, “Value constrained model-free continuous control,” 2019.
- [14] C. Gehring and D. Precup, “Smart exploration in reinforcement learning using absolute temporal difference errors,” in *Proceedings of the 2013 international conference on Autonomous agents and multi-agent systems*, pp. 1037–1044, 2013.
- [15] R. Koppejan and S. Whiteson, “Neuroevolutionary reinforcement learning for generalized helicopter control,” in *Proceedings of the 11th Annual conference on Genetic and evolutionary computation*, pp. 145–152, 2009.
- [16] P. Abbeel and A. Y. Ng, “Exploration and apprenticeship learning in reinforcement learning,” in *Proceedings of the 22nd international conference on Machine learning*, pp. 1–8, 2005.
- [17] H. Krasowski, X. Wang, and M. Althoff, “Safe reinforcement learning for autonomous lane changing using set-based prediction,” in *2020 IEEE 23rd International Conference on Intelligent Transportation Systems (ITSC)*, pp. 1–7, IEEE, 2020.
- [18] Y. S. Shao, C. Chen, S. Kousik, and R. Vasudevan, “Reachability-based trajectory safeguard (rts): A safe and fast reinforcement learning safety layer for continuous control,” *IEEE Robotics and Automation Letters*, vol. 6, no. 2, pp. 3663–3670, 2021.
- [19] T. Lew, A. Sharma, J. Harrison, A. Bylard, and M. Pavone, “Safe active dynamics learning and control: A sequential exploration-exploitation framework,” *IEEE Transactions on Robotics*, 2022. In Press.
- [20] A. K. Akametalu, J. F. Fisac, J. H. Gillula, S. Kaynama, M. N. Zeilinger, and C. J. Tomlin, “Reachability-based safe learning with gaussian processes,” in *53rd IEEE Conference on Decision and Control*, pp. 1424–1431, 2014.
- [21] S. M. LaValle, *Planning algorithms*. Cambridge university press, 2006.
- [22] S. Kousik, S. Vaskov, F. Bu, M. Johnson-Roberson, and R. Vasudevan, “Bridging the gap between safety and real-time performance in receding-horizon trajectory design for mobile robots,” *The International Journal of Robotics Research*, vol. 39, no. 12, pp. 1419–1469, 2020.
- [23] K. Leung, E. Schmerling, M. Zhang, M. Chen, J. Talbot, J. C. Gerdes,

- and M. Pavone, “On infusing reachability-based safety assurance within planning frameworks for human–robot vehicle interactions,” *The International Journal of Robotics Research*, vol. 39, no. 10-11, pp. 1326–1345, 2020.
- [24] Y. F. Chen, M. Liu, M. Everett, and J. P. How, “Decentralized non-communicating multiagent collision avoidance with deep reinforcement learning,” 2016.
- [25] Y. F. Chen, M. Everett, M. Liu, and J. P. How, “Socially aware motion planning with deep reinforcement learning,” 2018.
- [26] P. Long, T. Fan, X. Liao, W. Liu, H. Zhang, and J. Pan, “Towards optimally decentralized multi-robot collision avoidance via deep reinforcement learning,” 2018.
- [27] L. Tai, G. Paolo, and M. Liu, “Virtual-to-real deep reinforcement learning: Continuous control of mobile robots for mapless navigation,” in *2017 IEEE/RSJ International Conference on Intelligent Robots and Systems (IROS)*, pp. 31–36, IEEE, 2017.
- [28] L. Tai, J. Zhang, M. Liu, and W. Burgard, “Socially compliant navigation through raw depth inputs with generative adversarial imitation learning,” 2018.
- [29] Y. Ohta, H. Maeda, and S. Kodama, “Reachability, observability, and realizability of continuous-time positive systems,” *SIAM journal on control and optimization*, vol. 22, no. 2, pp. 171–180, 1984.
- [30] M. Althoff, *Reachability Analysis and its Application to the Safety Assessment of Autonomous Cars*. PhD thesis, Technische Universität München, 07 2010.
- [31] T. Koller, F. Berkenkamp, M. Turchetta, and A. Krause, “Learning-based model predictive control for safe exploration,” in *2018 IEEE conference on decision and control (CDC)*, pp. 6059–6066, IEEE, 2018.
- [32] A. Alanwar, A. Koch, F. Allgöwer, and K. H. Johansson, “Data-driven reachability analysis using matrix zonotopes,” in *Learning for Dynamics and Control*, pp. 163–175, PMLR, 2021.
- [33] L. K. Chung, A. Dai, D. Knowles, S. Kousik, and G. X. Gao, “Constrained feedforward neural network training via reachability analysis,” 2021.
- [34] N. Wagener, B. Boots, and C.-A. Cheng, “Safe reinforcement learning using advantage-based intervention,” *arXiv preprint arXiv:2106.09110*, 2021.
- [35] J. K. Scott, D. M. Raimondo, G. R. Marseglia, and R. D. Braatz, “Constrained zonotopes: A new tool for set-based estimation and fault detection,” *Automatica*, vol. 69, pp. 126–136, 2016.
- [36] V. Raghuraman and J. P. Koeln, “Set operations and order reductions for constrained zonotopes,” *arXiv preprint arXiv:2009.06039*, 2020.
- [37] S. Magdici and M. Althoff, “Fail-safe motion planning of autonomous vehicles,” in *2016 IEEE 19th International Conference on Intelligent Transportation Systems (ITSC)*, pp. 452–458, IEEE, 2016.
- [38] A. Shetty and G. X. Gao, “Predicting state uncertainty bounds using non-linear stochastic reachability analysis for urban gnss-based uas navigation,” *IEEE Transactions on Intelligent Transportation Systems*, 2020.
- [39] S. Vaskov, H. Larson, S. Kousik, M. Johnson-Roberson, and R. Vasudevan, “Not-at-fault driving in traffic: A reachability-based approach,” in *2019 IEEE Intelligent Transportation Systems Conference (ITSC)*, pp. 2785–2790, IEEE, 2019.
- [40] B. Amos and J. Z. Kolter, “Optnet: Differentiable optimization as a layer in neural networks,” in *International Conference on Machine Learning*, pp. 136–145, PMLR, 2017.
- [41] S. Dankwa and W. Zheng, “Twin-delayed ddpg: A deep reinforcement learning technique to model a continuous movement of an intelligent robot agent,” in *Proceedings of the 3rd International Conference on Vision, Image and Signal Processing*, pp. 1–5, 2019.
- [42] T. Haarnoja, A. Zhou, P. Abbeel, and S. Levine, “Soft actor-critic: Off-policy maximum entropy deep reinforcement learning with a stochastic actor,” 2018.
- [43] T. P. Lillicrap, J. J. Hunt, A. Pritzel, N. Heess, T. Erez, Y. Tassa, D. Silver, and D. Wierstra, “Continuous control with deep reinforcement learning,” 2019.
- [44] K. Chua, R. Calandra, R. McAllister, and S. Levine, “Deep reinforcement learning in a handful of trials using probabilistic dynamics models,” *Advances in neural information processing systems*, vol. 31, 2018.